Evolution of the Continental Lithosphere

Norman H. Sleep

*Department of Geophysics, Stanford University, Stanford, California, 94305-2215;
email: norm@pangea.stanford.edu*

Key Words   craton, platform, geotherm, xenolith, convection, stagnant-lid

■ **Abstract**   Stable cratons and stable continental platforms are salient features of
the Earth. Mantle xenoliths provide detailed data on deep structure. Cratonal litho-
sphere is about 200 km thick. It formed in the Archean by processes analogous to
modern tectonics and has been stable beneath the larger cratons since that time. Its
high viscosity, high yield strength, and chemical buoyancy protected it from being
entrained by underlying stagnant lid convection and by subduction. Chemically buoy-
ant mantle does not underlie platforms. Platform lithosphere has gradually thickened
with time as convection waned as the Earth's interior cooled. The thermal contrac-
tion associated with this thickening causes platforms to subside relative to cratons.
At present, the thickness of platform lithosphere is comparable to that of cratonal
lithosphere.

1. INTRODUCTION

Continental crust covers 40% of the Earth's surface. Plate tectonics nicely ex-
plains young fold mountain belts, but has less obvious implications in regions of
diffuse extension, such as the Basin and Range Province. This review is about the
passengers of the plates: the stable continents where very little happens.

I loosely subdivide the stable continents into cratons and platforms. From the
map of North America (Figure 1), the craton is the Canadian Shield where mainly
Archean (2.5 Ga and older) rocks outcrop. The basement of platforms is younger
and often buried by a few kilometers of sedimentary rocks. The ∼1.1 Ga Grenville
Province outcrops mainly between the Appalachians and the craton, whereas to
the west, it is beneath platform sediments. The regions west of the Rockies and
east of the Appalachians have been active in the past 300 million years (m.y.). I
conclude that the difference between platforms and cratons extends down to the
base of the lithosphere.

Fei et al. (1999) and Jones et al. (2003) have edited symposium volumes on
the observational and petrological aspects of stable lithosphere. Sleep (2003a,b)
discussed the dynamics. I cannot discuss all the observations in detail but rather
concentrate on broad aspects that relate observable tectonics to geodynamics.
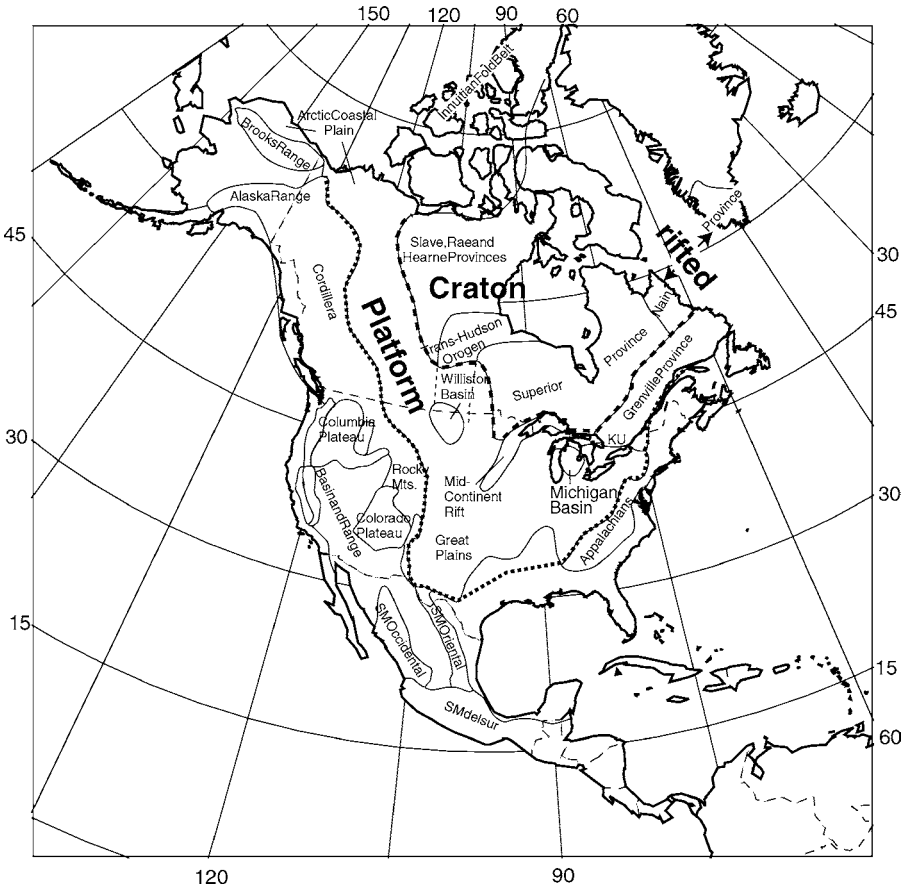
Figure 1   Simplified geological map of North America (modified after Chulick & Mooney 2002). Dotted line separates platform from the orogens to the east, south, and west. Dashed line separates craton from platform. Note the rifted craton of the Nain Province in Baffin Bay and the Michigan basin with several kilometers of platform subsidence.

2. CRATONAL LITHOSPHERE

The cratonal lithosphere extends to a depth of about 200 km. Until recently, earth scientists did not have a good way to quantify this depth. They used seismology and heat flow. Mantle xenoliths from diamond pipes (kimberlites sensu latu) now provide more precise data (Figure 2). Strictly speaking, the data constrain the geotherm on the day and place of the eruption.

2.1. Heat Flow within the Lithosphere

The xenolith geotherm is a good starting point from which to discuss cratons. The xenoliths give the heat flow through the rigid part of the mantle lithosphere. The
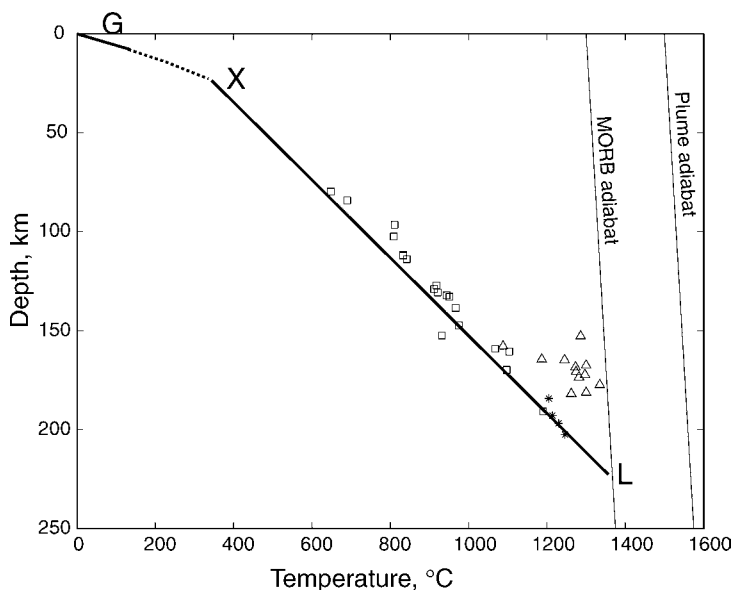
Figure 2 The xenolith geotherm beneath the Slave Province in Canada. Data from
the Jericho kimberlite by Kopylova et al. (1999) using the pressure-temperature formu-
lation of Brey & Köhler (1990) and converted to depth by Sleep (2003b). Squares are
unsheared xenoliths, triangles are sheared xenoliths, and asterisks are megacrystalline
xenoliths. The conductive geotherm in the mantle extrapolates to the base of the crust
at point X and to the MORB adiabat at point L. The shallow geotherm G is measurable
in boreholes.

array is linear within error (Figure 2). The conductive heat flow is

$$q = k\frac{\partial T}{\partial Z}, \tag{1}$$

where k is the thermal conductivity, T is temperature, and Z is depth. The geotherm
is nonlinear if the conductivity is not constant, if the lithosphere is not in steady
state, or if there is significant radioactive heat generation. For example, at steady
state,

$$\frac{\partial q}{\partial Z} = -Q, \tag{2}$$

where Q is radioactive heat generation per volume. It is futile to attempt to resolve
slight variations of conductivity and the feeble amount of radioactive heat gener-
ation in the mantle from these data. There is good hope of recognizing nonsteady
states, especially in regions such as southern Africa where kimberlites erupted
over a period of time (Bell et al. 2003, Griffin et al. 2003b).

   In detail, the low-temperature envelope is probably the best estimate of the
geotherm. The kimberlite magmas sometimes pond and partly crystallize at depth.

They can heat their surroundings but not cool them. The megacrystalline xenoliths in Figure 2 crystallized from ponded kimberlite magma. However, the volume of kimberlites is trivial, a few cubic kilometers. These rare intrusions have negligible direct effects on the long-term temperature of the lithosphere.

The xenolith geotherm does not extrapolate to the surface temperature, ~0°C. Rather, the crustal geothermal gradient is higher than the mantle gradient (Figure 3). This occurs because the thermal conductivity of hard crustal rocks is less than mantle conductivity (Equation 1, 2.4 versus 3.0 W m^{-1} K^{-1}). There is significant radioactive heat generation in the crust, so the surface heat flow is higher than the heat flow at the base of the crust (Equation 2).

The thermal transition from lithosphere to underlying mantle is gradual (Figure 4). A convenient scale depth is that where the conductive geotherm extrapolates into the underlying adiabat. It has the advantage that one determines it from the xenolith geotherm without needing really deep xenoliths. However, the methods for obtaining pressure and temperature from xenoliths may have
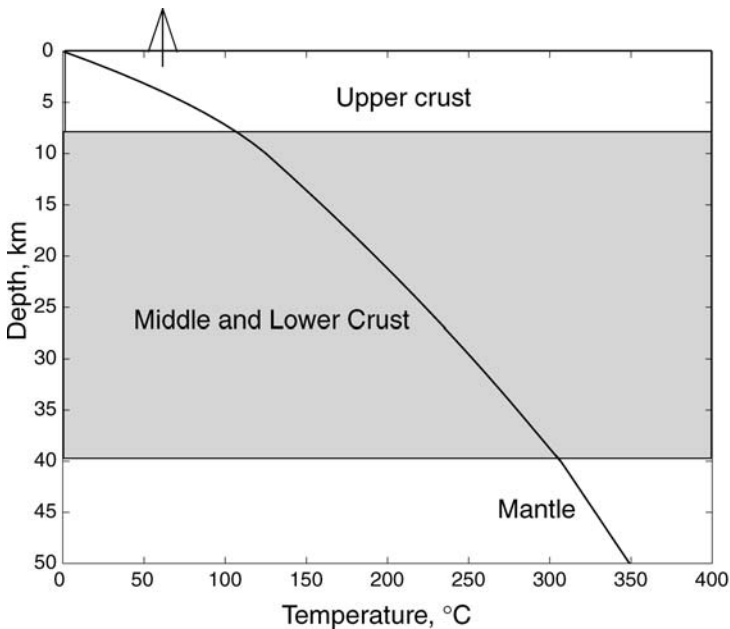

Figure 3 Schematic diagram of the geotherm in the continental crust. The geothermal gradient becomes less steep with depth because radioactive heat generation in the crust causes heat flow to decrease with depth. In practice, the heat flow near the surface and the radioactive heat generation in the upper ~10 km of the crust are well constrained. The radioactivity in the rest of the crust is poorly constrained. It is therefore difficult to extrapolate the surface geotherm into the mantle. The thermal gradient is lower in the mantle than in the deepest crust because the mantle conductivity is higher.
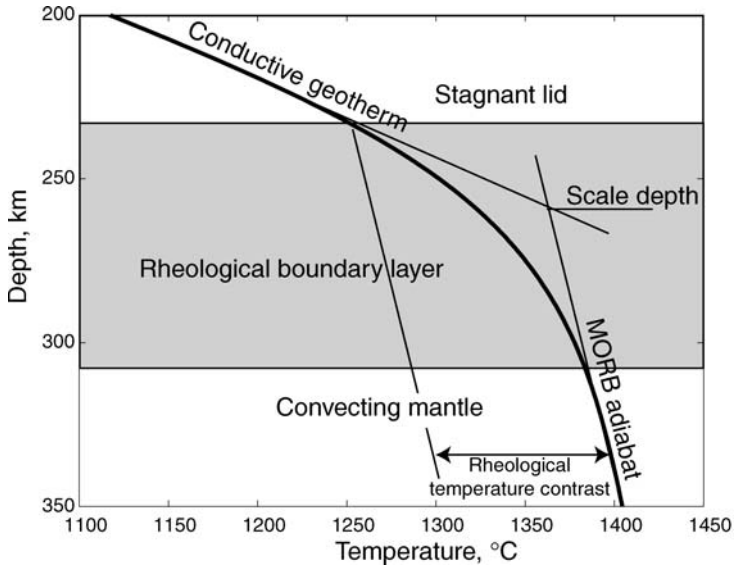
Figure 4   Schematic diagram of the rheological boundary layer. The geotherm (*thick line*) goes from the conductive geotherm in the stagnant lid to the MORB adiabat at the base of the boundary layer. The rheological temperature contrast is the difference between the temperature at the top of the boundary layer and the MORB adiabat.

systematic errors and not be internally consistent with the methods for obtaining the abiabat from mid-oceanic ridge basalts (MORB) (see Bell et al. 2003). Globally the scale depth of cratonal xenolith geotherms is relatively uniform, around 200 km (Rudnick & Nyblade 1999). There are thinner small cratons, like Tanzania (Chesley et al. 1999) and West China (Gao et al. 2002), but no grossly thicker ones. The gross lithospheric thicknesses and their relative variations are fine, but the absolute uncertainty on the base of the lithosphere (as defined) is around 25 km.

The transition zone between rigid lithosphere (the stagnant lid) and convecting mantle is the rheological boundary layer. Both convection and conduction carry heat in this region. The geothermal gradient goes from conductive above to convective (abiabatic) below. The dynamics of this region control the long-term thermal state of the lithosphere (see section 3).

Before the advent of the xenolith geotherm, one procedure for obtaining lithospheric thickness was to measure the shallow geotherm to get surface heat flow from Equation 1. The regional correlation of heat flow and heat generation and gravity data gave some indication that the shallow crustal rocks with high radioactive heat generation extend to a depth of 7–10 km. There are few good constraints on the radioactivity of the rest of the crust other than that it is somewhat lower than that in the upper crust. For simplicity, I define the heat flow generated by

radioactivity to be

$$q_{rad} \equiv Q_{crust} Z_{crust}, \tag{3}$$

where Q_{crust} is the average radioactive heat generation in the crust and Z_{crust} is the thickness of the crust. The heat flow coming out of the mantle q_{man} is the measured surface heat flow q_{surf} minus the radioactive heat flow. In a more careful application using Equation 1, the thickness of the lithosphere is in compact form

$$Z_{lith} = \frac{k(T_{lith} - T_{rad})}{q_{surf} - q_{rad}}, \tag{4}$$

where T_{lith} is the temperature at the base of the lithosphere and T_{rad} is the temperature to which the conductive mantle geotherm extrapolates at the surface. The procedure works tolerably when the difference between the heat flows is large, but becomes unstable when the difference is small. Thus, compilations based on heat flow yield lithospheric thicknesses up to 400 km (Artemyeva & Mooney 2001).

Technology exists to measure radioactive decay in the crust and mantle directly by detecting antineutrinos from the uranium and thorium decay chains (Fiorentini et al. 2003). Potassium decay is much harder to detect. However, no detectors are in operation within cratons. The instruments require deep mines and costly logistics.

Seismology constrains the base of the lithosphere. However, seismic velocity is not a simple function of temperature if small amounts of melt are present in the rheological boundary layer and the underlying mantle. It is thus unclear how to relate the base of the seismic lithosphere to detailed thermal and chemical structure.

Poor resolution is a major problem with seismic data. The high-velocity region of the mantle lithosphere clearly extends down to ∼200 km. In may appear to extend down further in inversions for seismic velocity. A stable definition is to take the base of the seismic lithosphere at the depth where its difference from ordinary mantle ceases to be resolved. It is then shallower than 250 km (Simons et al. 1999, Röhm et al. 2000, Ritsema & van Heist 2000). Seismic studies constrain the seismic structure in southern Africa well enough that it can validate and laterally extend xenolith data (Shirey et al. 2003).

2.2. Antiquity and Stability of the Cratonal Lithosphere

In addition to defining the geotherm, xenoliths provide information on the antiquity and survival of cratonal lithosphere. Dating of diamond inclusions and other xenoliths indicates that 150- to 200-km-thick lithosphere existed beneath southern Africa in the Archean (Boyd et al. 1985). Osmium isotope studies confirm that cratonal lithosphere has remained stable for at least the past 2 Ga (Carlson et al. 1999, Pearson 1999). For example, the lithosphere beneath Somerset Island, Canada, has remained stable to a depth of 150 km since the Archean (Schmidberger et al. 2002, Irvine et al. 2003). Saltzer et al. (2001) showed that Archean xenoliths from a depth of 180 km beneath southern Africa have remained in place. Shirey et al.

(2003) and Griffin et al. (2003b) provide detailed studies showing that this depth is representative but varies regionally correlating with surface geology.

Deep crustal xenoliths constrain the time at which the cratonal geotherm approached its current value. Such work is just beginning. In southern Africa, it appears that platform and cratonal regions had similar geotherms from 0.6–0.8 Ga to the Jurassic (Schmitz & Bowring 2003). The geotherm had approached its current value in the southern Slave Province by 1.8 Ga (Davis et al. 2003a).

Archean and younger mantle xenoliths show a strong imprint of subduction. (e.g., Saltzer et al. 2001; Shulze et al. 2003a,b; Jacob et al. 2003; Menzies et al. 2003). Sulfur-33 isotope anomalies in diamonds (Farquhar et al. 2002) are particularly strong evidence of Archean subduction. These rocks came from material subducted before there was significant oxygen in the air (Pavlov & Kasting 2002).

The straightforward inference is that xenoliths provide an in-place record of Archean processes in the deep lithosphere. A second key inference is that the Archean lithosphere, once stabilized, has remained beneath its Archean crust. Detailed comparison of seismic and xenolith data supports both inferences in southern Africa (Shirey et al. 2003), as do more limited data from the Slave craton (Davis et al. 2003b). The overall correlation of surface geology and xenolith geology is good. Cratonal lithospheric mantle like the crust experiences discrete events, such as those associated with plumes, continental break-up, and subduction (Griffin et al. 2003a,b; Shirey et al. 2003; Bleeker 2003).

Thus, I expect that a field geologist would find Archean mantle lithosphere as complicated on a map and outcrop scale as Archean basement. Mantle lithosphere appears simple in seismic studies because of poor resolution. Individual xenoliths give sparse detailed information.

I expect that much more information will become available from xenoliths. For example, the emplacement ages of many kimberlites are now reliable (Heaman et al. 2003). Multiple episodes occur in several areas making possible a time history of the mantle geotherm (Bell et al. 2003). Zoned diamonds with inclusions are a potential source of information (Schulze et al. 2003a). It may be possible to associate dated inclusions with zones in the diamond. For example, it may be possible to constrain the movement of a piece of lithosphere in P-T space as predicted by dynamic models (O'Neill & Moresi 2003). As already noted, studies of lower crustal xenoliths constrain the evolution of the mantle geotherm through time.

2.3. Buoyancy of Archean Mantle Lithosphere

The buoyancy of cratonal lithospheric mantle aids its longevity. Seismic and xenolith studies indicate that buoyant material exists both locally and regionally at depth (Griffin et al. 2003b, Shirey et al. 2003). A combined approach of adding isostasy to estimate elevation and geoid confirms that cratonal lithospheric mantle is regionally buoyant, but cannot provide clear resolution of its base (Shapiro et al. 1999a,b; Mooney & Vidale 2003). I present the formalism because I need it in section 3.5 for discussing freeboard. Overall the results are compatible with a density deficit of $\sim$50 kg m^{-3} from xenolith studies used by Doin et al. (1997)

and Sleep (2003a) in dynamic models from petrological considerations (Griffin et al. 1999). Lenardic et al. (2003) used 100–200 kg m^{-3} in their models.

I present isostasy conceptually so that I do not obscure the basic issues. The ridge axis is a convenient reference point for isostasy on the modern Earth. The elevation of a continental region above the ridge axis in linearized form depends on the integral

$$E = \left\lfloor \frac{\rho_m}{\rho_m - \rho_w} \right\rfloor \int \left\lfloor \frac{\Delta\rho_C}{\rho_m} - \frac{\rho_{ref}\alpha\,\Delta T_C}{\rho_m} \right\rfloor dz, \qquad (5)$$

where ρ_m is the density of the mantle compensating layer, ρ_w is the density of ocean water for the part of the elevation difference below water (or the density of air for the exposed elevation), $\Delta\rho_C$ is the chemical density-deficit or continental lithosphere (including the crust) relative to oceanic lithosphere, ρ_{ref} is a reference density, α is the volume thermal expansion coefficient, ΔT_C is the temperature of continental lithosphere below that of an adiabat at the ridge axis, and z is depth. Typically, continental crust and lithosphere are chemically less dense than the column beneath the ridge axis, but are cooler. The chemical effect is greater so that ridge axes are ~2.5 km below sea level.

Continental elevation is higher than expected from just its crustal structure and a thermal base around 200-km. This requires a chemical buoyancy region within lithospheric mantle in addition to the obvious buoyancy in the crust. The chemical buoyancy in the deep lithosphere to the first order counteracts its negative thermal buoyancy. The geoid height provides a second relationship that constrains the depth of this buoyant region. Geoid height is proportional to the integral of density contrast times depth,

$$U \propto \int \left\lfloor \frac{\Delta\rho_C}{\rho_m} - \frac{\rho_{ref}\alpha\,\Delta T_C}{\rho_m} \right\rfloor z\,dz, \qquad (6)$$

where geoid height is relative to that at the ridge axis. The intraplate stress-resultant F (in units of stress per length with tension positive) relative to the rigid axis is proportional to the same integral. Geoid data indicate that the buoyant region extends deep within the lithosphere, but an integral constraint cannot resolve the details of the base of the lithosphere. Another difficulty in applying isostasy is that glacial rebound and deep convection (including slabs) in the mantle have significant effects on the geoid that must be distinguished from lithospheric effects.

2.4. Tectonics of the Formation of Archean Lithosphere

Archean lithosphere is different from lithosphere that formed later in the Earth's history. In fact, petrologists use chemical differences to tell where younger lithosphere underlies cratons (e.g., Canil et al. 2003, Griffin et al. 2003a). Archean lithosphere is more buoyant and has olivine with higher magnesium numbers (that is, a lower fraction of ferrous iron) than normal mantle. It is depleted in basaltic

and volatile components relative to normal mantle except where they have been added by later events or by material subducted in the Archean.

The present Archean provinces are the remnants of larger blocks. Bleeker (2003) identifies 35 major pieces, all bound by break-up margins. Break-up began in the Archean and has continued to the present. For example, the Baffin Bay and the North Atlantic rift the Nain province between Labrador, Greenland, and Scotland (Bleeker 2003) (Figure 1). Various blocks have collided at subduction zones, sometimes forming larger shields. Such collisions began in the Archean and continue to the present. Bleeker (2003) has made some progress in reconstructing the larger blocks that existed at the end of the Archean. These may be somewhat smaller than current continents.

Overall, Archean tectonics resembles modern plate tectonics. All Archean tectonic discussions involve events, not a continuous flow of seething fluid crust. In particular, the base of the Archean crust was solid most of the time (Burke & Kidd 1978). Crust-derived melts erupt only occasionally. I have already mentioned subduction, continental break-up, and continental extension. There is evidence of Archean strike-slip faulting and intracontinental extension. Plumes are discussed at the end of this section and in section 2.5, together with chemical constraints.

Major strike-slip faults are good evidence of plate tectonics, at least in the sense of rigid plates and weak boundaries (Sleep 1992). Physically the horizontal motion on strike-slip faults provides no gravitational driving force but some resistance to plate motion. They can exist only if they are weak enough that their resistance is unimportant in the plate-wide force balance.

Archean strike-slip faults are likely to be more common than reported (Chen et al. 2001). Vertical tectonics along mainly strike-slip faults is often more evident in the field than the predominant strike-slip motion. Well-documented Archean strike-slip faults occur in the Yilgarn craton of Australia (Chen et al. 2001) and the Pilbara craton of Australia (Kiyokawa et al. 2002; Zegers et al. 1998, 2001).

Some modern strike-slip faults take up the oblique component of motion along arcs or, like the San Andreas, grow at the expense of an arc after the passage of a Mendocino-type triple junction. Such faults are hard to spot in ancient rocks because they are parallel to the gross geological strike. They are most likely to be preserved when they are mildly transpressional. Significant compression leads to deep erosion and significant extension to deep burial and later compressional tectonics.

The Inyoka fault in southern Africa has these requisite features, even though no one has associated it with the initiation of a San Andreas-type fault with Mendocino- and Rivera-type triple junctions. I discuss it because as the oldest documented strike-slip (Heubeck & Lowe 1994) fault at ∼3200 Ma. Enough of its length remains that it is productive to invoke plate tectonics. As with the San Andreas, it cuts syntectonic basins, here of the Moodies Group (Heubeck & Lowe 1994, de Ronde & de Wit 1994). Moodies-time tectonics are associated with nearby extensional detachment faulting as would occur near a ridge-trench-fault (Rivera) triple junction (Heubeck & Lowe 1994, Kisters et al. 2003). The fault separates

similar-looking terrains that cannot be matched when mapped in detail as do major faults in the San Andreas system that are basically parallel to gross strike (de Ronde & de Wit 1994, de Ronde & Kamo 2000).

Strike-slip faults provide indirect evidence on plate size as they resolve the oblique component of motion. With large modern plates, the sense of oblique slip remains constant for tens of million years until a triple junction passes. The southern Superior province in Canada exhibits this feature (Sleep 1992).

Core-complex-like extension, as already noted, occurred at Moodies Group time, ~3200 Ma, in southern Africa (Heubeck & Lowe 1994, Kisters et al. 2003). The Split Rock Shear zone in the Pilbara block is a ~3450 Ma core complex feature (Zegers et al. 2001).

The global importance of vertical tectonics in the Archean has not been sorted out. The 500-km wide Minto block in the northeastern Superior province is an example (Bédard et al. 2003). This region is wider than modern hot compressional orogens. The Basin and Range province provides a modern analogy where a mantle plume heats the middle and lower crust to the point that they behave as a fluid. A broad region of folding would occur in the Basin and Range province if it came under compression. This would trigger vertical tectonics if dense supracrustal rocks overlaid less dense, easily mobilized granitic rocks. Such unstable stratification occurs now in the Columbia plateau. Clearly, the higher temperatures of Archean normal mantle and plumes would make this foundering more likely than at present.

The high temperature of the Archean mantle also made oceanic basaltic plateaus with >20-km thick crust more common than today. Remelting of this crust under hydrous conditions forms siliceous magmas. Bédard et al. (2003), for example, start the Minto block with a broad oceanic plateau.

2.5. Chemical Mass Balance

How Archean crust and lithospheric mantle formed is still subject to debate, although there were processes analogous to the present including vertical tectonics within hot crust. I will now review mass balance constraints to show that the crust-forming processes are not simply related to those forming the mantle lithosphere. This may be surprising in that, once stabilized, Archean lithospheric mantle tends to stick with its overlying crust.

Archean continental lithospheric mantle is to the first order the residuum of high-percent partial melting of hot mantle. The resulting melt, komatiites, are very magnesian. In detail, lithospheric mantle samples are not simple residua of Archean komatiites (Francis 2003), but the first-order hypothesis illustrates the mass balance issues. Continental crust is obviously not composed of komatiites (e.g., Herzberg 1999). The problem gets worse with highly incompatible trace elements including the radioactive elements K, U, and Th. The continental crust contains ~35% of the total "bulk silicate earth" (BSE) supply. But as the crust is only 0.5% of the mass of BSE, it is enriched by a factor of ~70 in K, U, and Th relative to BSE. This implies that at least 35% of the BSE passed through whatever

melting processes eventually formed the continents. These constraints apply even though some crust has formed since the Archean and some Archean crust has been subducted. It is not obvious whether formation or subduction dominated or equivalently whether the mass of continental crust has grown or shrunk since the Archean (see Jacobsen 1988, McLennan & Taylor 1991).

A two-stage process suffices for the mass balance of major elements in the crust. Basalt erupts as a primary melt from the mantle and becomes hydrated in analogy to modern ridge basalts. It later remelts either at the top of the subducted slab or within nascent (oceanic plateau or primitive arc) continental crust to form quartz-bearing igneous rocks. The higher temperature of the mantle made partial melting more common in these environments than in the modern Earth.

An additional ingredient is needed to explain trace elements. The rare earth element pattern of average continental crust from clastic sediments is enriched in light rare earths and flat in heavy rare earths (McLennan & Taylor 1991). A mixture of a flat rare earth source from oceanic crust and plateaus and one from low-percent partial melts, like modern alkalic basalts that are strongly enriched in light rare earths and depleted in heavy ones, would produce this pattern. The alkalic component may have added much of the K, U, and Th to the crustal mixture.

The final crust is complicated because it continued to remelt and mix after it left the mantle. Supracrustal rocks ended up deep in the crust. Water-soluble components, like Sr and Rb, behaved differently in weathering and hydrothermal alteration from rare earth elements and the bulk mass of the rock.

The converse problem exists with the mantle lithosphere. It is about 2% of the BSE, and the Archean mantle lithosphere is less than 1%. Komatiites form from 30% to 50% melting in anhydrous conditions (Arndt 2003). (33% partial melting gives 1 part komatiite to 2 parts residuum; 50% melting gives 1 to 1.) The Archean lithospheric mantle is thus the residual product of melting less than 2% of the BSE. Most of the >35% of the BSE that melted in the Archean to ultimately yield continental crust produced residuum that ended up back in the normal mantle, not in the lithosphere. This is evidence for vigorous mantle circulation that is akin to plate tectonics.

3. HEAT TRANSFER NEAR THE BASE OF THE LITHOSPHERE

How does Archean lithosphere persist since it was stabilized? There is a sampling problem here in that we can study only the cratons that survived. Furthermore, phenomenological analyses are difficult because we do not have many large cratons. The common thickness, 200 km, of many cratons, the establishment of this thickness early in their evolution, and the feeble extent of crustal and mantle tectonics since that time are salient features that any geodynamic model needs to explain.

I condense notation in examples by ignoring the existence of the continental crust and making the lithosphere a homogeneous region of conductivity $k = 3$ W m^{-1} K^{-1}, thermal diffusivity $\kappa = 0.75 \times 10^{-6}$ m^2 s^{-1}, unperturbed

mantle density $\rho = 3400$ kg m^{-3}, and volume thermal expansion coefficient $\alpha = 3 \times 10^{-5}$ K^{-1}. Because these parameters do not vary much with depth and temperature and are well enough constrained compared with viscosity, it is convenient to consider them the given constants. The linear conductive geotherm within the lithosphere extends between the potential temperature of 0°C at the surface and T_L and the base depth of the lithosphere Z_L. I use 1300°C and 200 km, respectively, in example calculations.

3.1. Maintaining Cratonal Lithosphere Heat Flow

Cratonal lithosphere is about 200 km thick. To the first order, it is in thermal steady state where the laterally averaged heat flow at its base equals the laterally averaged heat flow into the crust. There is considerable time averaging of bottom process by surface heat flow since the thermal time constant $Z_L^2/\pi\kappa$ (defined as the time for a conductive half space to reach the steady-state heat flow through the stagnant lid) is 540 m.y. (Choblet & Sotin 2000, Nyblade & Sleep 2003). Conversely, the time constant is short compared with the crustal age. The lithosphere would be ~600 km thick, more like the Moon, if only conduction occurred.

Stagnant-lid convection driven by local temperature contrasts with the rheological boundary layer is the most likely mechanism for heat flow into the base of the lithosphere (Sleep 2003a). Plumes are insufficient, and their aftermath retards stagnant-lid convection (Nyblade & Sleep 2003). Drag at the base of the plate is also insufficient and implies, contrary to observations, that wider cratons have thicker lithosphere (Sleep 2003a).

Solomatov & Moresi (2000) developed an elegant "parameterized" convection formulation by extending the results of Solomatov (1995) and Davaille & Jaupart (1993a,b). For simplicity, I consider a temperature- and chemical-dependent viscosity

$$\eta = \eta_0 \left[\frac{\eta_C}{\eta_0}\right]^\phi \exp\left[\frac{\Delta T}{T_\eta}\right], \tag{7}$$

where η_0 is the viscosity of normal mantle at a reference adiabat, η_C is the viscosity of chemical lithosphere at the reference adiabat, ΔT is the temperature below that adiabat, T_η is the temperature scale for viscosity, and the fraction of chemical lithosphere at a "point" in the mantle ϕ varies from 0 to 1. Doin et al. (1997), Sleep (2003a,b), and Nyblade & Sleep (2003) used this formulation in numerical models. The steady state laterally averaged heat flow in terms of material parameters (in the absence of chemical buoyancy) is

$$q_{SS} = (a + bn)kT_\eta^{2(n+1)/(n+2)}(\alpha\rho g)^{n/(n+2)}(\kappa\eta_0)^{-1/(n+2)}\tau_{\text{ref}}^{(n-1)/(n+2)}, \tag{8}$$

where a and b are dimensionless constants, n is the exponent of the nonlinear power-law rheology, and τ_{ref} is a constant with dimensions of stress (Solomatov & Moresi 2000). One recovers the familiar Newtonian or linear viscosity for $n = 1$.

Following Richter (1988) and Sleep (2003), Equation 8, with 7 for the viscosity, yield the lithospheric thickness as a function of mantle temperature. The convecting mantle has cooled over time. Abbott et al. (1994) give decrease of 150 K in the last 3 Ga; Galer & Mezger (1998) compile this as their preferred estimate. Grove & Parman (2004) give 100 K. Their estimate is based on the inference that komatiites were hydrous melts. This seems unlikely (Arndt 2003), but the problems remain with regard to inferring mantle source temperature from petrology and distinguishing plume-related from normal-temperature sources.

If we normalize to the current lithospheric thickness Z_{now} and mantle heat flow, the only uncertain parameters are the temperature decrease since the Archean ΔT_A, the power n, and the temperature scale T_η. The Archean lithospheric thickness to the first order is

$$Z_A = \frac{kT_L}{q_{SS}} = Z_{now} \exp\left[\frac{-\Delta T_A}{(n+2)T_\eta}\right]. \tag{9}$$

I have already noted that the Archean lithosphere achieved nearly its present thickness soon after it stabilized. This requires that the power n be large (strongly stress-dependent viscosity) and/or that the scale temperature T_η be large (weakly temperature-dependent viscosity). The alternative is that the presence of a chemically buoyant layer controlled lithospheric thickness over time, which is considered in the next section.

The temperature contrast across the rheological boundary layer is a second observable parameter. In terms of physical parameters, it is simply

$$\Delta T_{rheo} = 1.2(n+1)T_\eta \tag{10}$$

(Solomatov & Moresi 2000). This parameter is measurable from a xenolith geotherm (Figure 5). It would help to have xenoliths from all depths, but one can
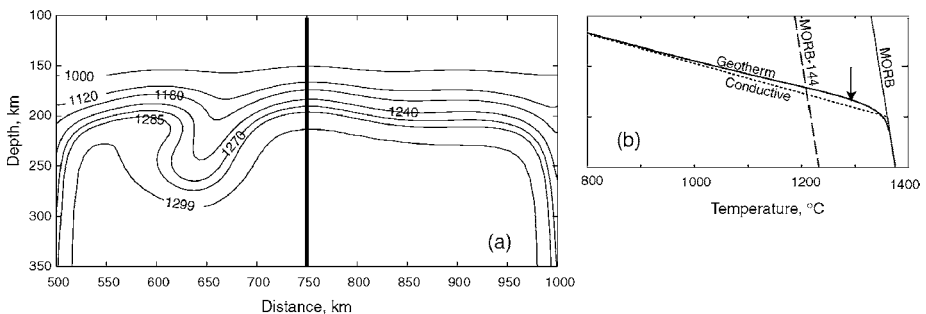

Figure 5   Potential temperature contours show convection beneath a stagnant lid (*a*). The dark line shows the position of the geotherm sampled in panel (*b*). From theory in Equation 10, the rheological boundary contrast should be 144 K. This quantity would be obtained from the laterally averaged temperature. The computed geotherm, however, has a break in slope at only ~70 K (*arrow*). From model in figure 1 of Sleep (2003b).

constrain ΔT_{rheo} from the data in hand (Figure 2). Some care is needed because a kimberlite provides a point measurement rather than the laterally averaged geotherm in Figure 4. The numerical geotherm from Figure 5 comes from an upwelling near a nascent downwelling, a plausible place for a kimberlite to start. The local geotherm is hotter than the laterally averaged geotherm, but one would not know this from real data from a single kimberlite. The break in the geotherm from linearity is measurable, and one would get about half the predicted rheological temperature contrast by doing this. The data in Figure 2 show no break in slope to within 100 K of the MORB adiabat, suggesting that the rheological temperature contrast is less than 200 K.

This constraint cannot be satisfied along with the constraint from Equation 8 that the lithospheric thickness did not change much with time. Using the last 2500 Ma, where the temperature change is 125 K and the maximum value 200 K of the rheological contrast in Equation 10, yields an Archean lithosphere that was 53% and 60% of the modern thickness for $n = 5$ and $n = 1$, respectively. These unacceptable results depend weakly on the exponent n. Sleep (2003a) obtained models with much more complicated contrived rheologies that satisfied both constraints. Further work on the effects of complicated rheology should have a strong basis in mineral physics. The mundane hypothesis of the existence of chemically less dense lithosphere is the probable reason that Archean lithosphere maintained its thickness over time.

3.2. Convection Beneath Chemically Buoyant Lithosphere

I now shift to how chemically lithosphere may persist over time. To affect convection, the buoyant lithosphere must extend downward into the temperature range that would normally be occupied by the rheological boundary layer (Figure 6). I do not have good parameterized theory for convection beneath a buoyant chemical lid, but a trial expression for the rheological temperature contrast beneath the chemical layer for a linear rheology is

$$\Delta T_{\text{rheo,C}} = \Delta T_{\text{rheo,0}} \left\lfloor \frac{q_{SS,C}}{q_{SS,0}} \right\rfloor^{3/4}, \tag{11}$$

where the subscript C indicates convection beneath the chemical layer and the subscript 0 indicates convection beneath lithosphere made of normal mantle. An expression of this form can be obtained from local Rayleigh number systematics (see Lenardic & Moresi 2003). The exponent for the heat flow ratio for a nonlinear rheology is $(n + 2)/2(n + 1)$, which is weakly dependent on n. It is $7/12$ for $n = 5$.

Equation 11 includes only potentially measurable quantities. We know the heat flow through the chemical lithosphere $q_{SS,C}$ from the xenolith geotherm, and we might find the rheological temperature contrast, albeit with more difficulty. For now, I use platform lithosphere as a place where steady-state convection occurs beneath normal mantle. (Old oceanic lithosphere is another choice.) We can get both the heat flow and the rheological temperature contrast if we are fortunate to find mantle xenoliths in our platform. Then we could, in principle, get the power n,
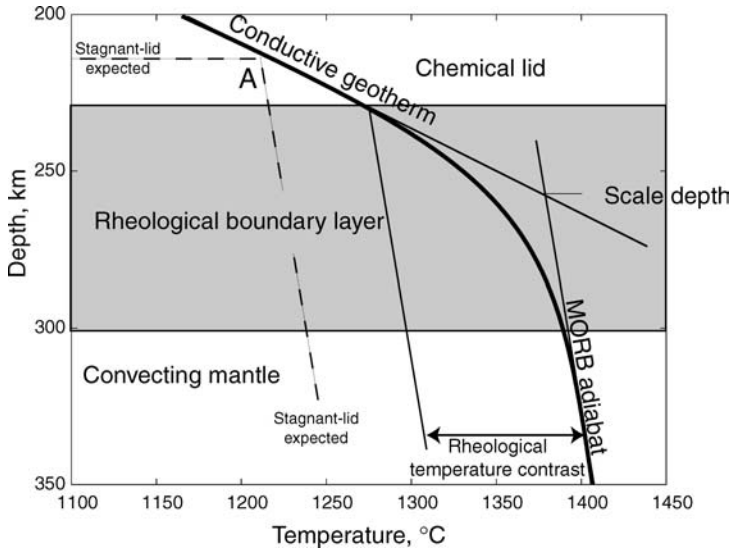
Figure 6 Schematic diagram of the rheological boundary layer beneath a chemically buoyant lid. The rheological temperature contrast is less than it would be without a chemical lid for ordinary stagnant-lid convection. The top of the rheological boundary layer then would be at temperature-depth point A.

but, in practice, this is futile given its weak presence in Equation 11. Overall it may be hard to apply Equation 11 if platform heat flow is essentially the heat flow through chemical lithosphere. This implies that we live in a time where the chemical layer is just losing its effect on convection. I return to the implications of this inference in sections 3.4 and 3.5.

I now consider the survival of a chemical layer above a convecting half space. The chemical layer needed to be buoyant enough that it did not catastrophically overturn into the mantle. This catastrophe requires that dimensionally $\Delta T_{\text{rheo}} \rho \alpha \geq \Delta \rho_C$, which implies for my parameters that ΔT_{rheo} is greater than 490 K. This situation conflicts with the xenolith geotherm. I need not consider this case further, as it obviously did not happen with the existing cratons.

I do need to consider the gradual entrainment of wisps of the buoyant material into the underlying much more viscous half space (Figure 7). Plate drag is likely to align the convection cells into rolls (Richter 1973). Rolls are more effective entrainers than plume-like downwellings (e.g., Davaille et al. 2002). The laterally averaged thinning rate of the chemical lithosphere is dimensionally

$$-\frac{\partial Z_C}{\partial t} = q_{SS,C} \left\lfloor \frac{\rho \alpha}{2 \rho C \Delta \rho_C} \right\rfloor, \tag{12}$$

where $\Delta \rho_C$ is the density contrast of chemical lithosphere relative to normal mantle (Sleep 2003a). This equation provides a reasonable estimate of the actual
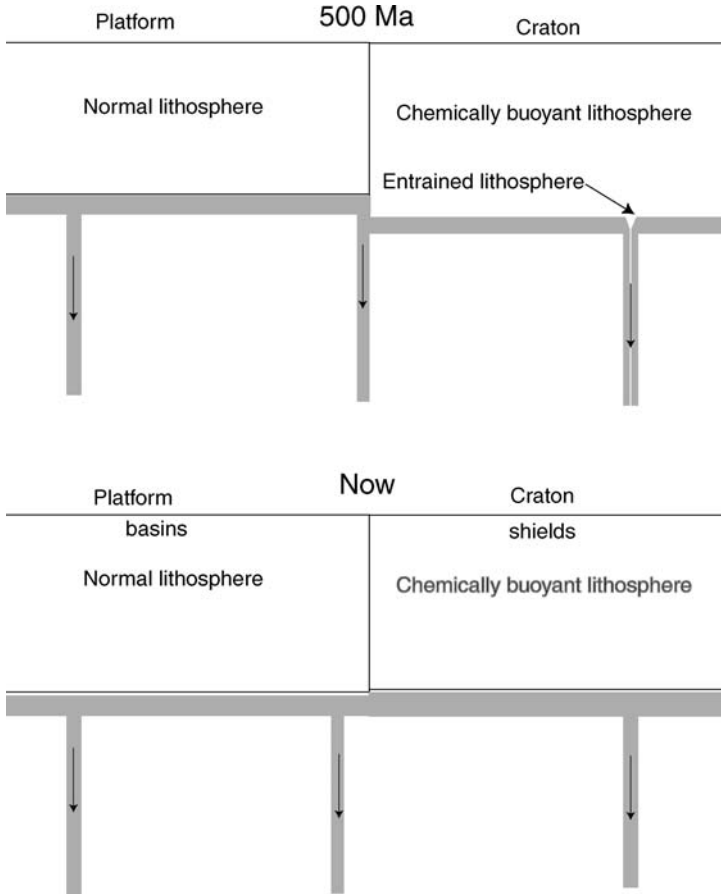
Figure 7 Schematic diagram of convection beneath a platform (*left*) and a craton (*right*) at 500 Ma (*above*) and now (*below*). At 500 Ma, stagnant-lid convection controlled platform lithosphere thickness while chemical buoyancy controlled cratonal lithosphere thickness. Platform lithosphere thickened with time as the Earth's interior cooled. Cratonal and platform lithosphere now have similar thicknesses. The platform subsided as it cooled forming basins while the craton has exposed shields. Note that convective downwelling entrains thin wisps of buoyant lithosphere at 500 Ma. Entrainment waned as the rheological boundary layer moved beneath the base of the chemical lithosphere.

entrainment when viscosity does not depend on chemistry $\eta_C = \eta_0$. It contains no poorly constrained parameters. The predicted entrainment rate is ∼100 km per billion years, which is grossly excessive. Chemical buoyancy alone does not keep the chemical lithosphere in place (Doin et al. 1997, Sleep 2003a). These models also confirm that catastrophic turnover does not happen for realistic parameters.

To persist, the chemical lithosphere needs to be so viscous that high viscosity rather than buoyancy resists entrainment. The entrainment rate then depends inversely on the viscosity ratio η_C/η_0 (Davaille et al. 2002). Numerical modeling is difficult in that it does not easily resolve the thin wisps of entrained material. The minimum viscosity ratio is 20, which applies if viscosity is not strongly temperature dependent $T_\eta = 100$ K (Doin et al. 1997, Sleep 2003a). The ratio would have to be much higher if viscosity changes an order of magnitude per 100 K, but numerical models have yet to resolve the precise amount.

Cratonal lithosphere may conceivably lose its viscous or buoyant identity from normal mantle by metasomatism by fluids or by intrusion of mafic dikes. Combined xenolith and seismic work shows that an extensive zone of major and trace element refertilization exists in the deep lithosphere beneath the Protenozoic Bushveld Complex (Hoal 2003).

Kimberlite intrusions may decrease viscosity by increasing volatile content without affecting density and seismic velocity. I discuss an example of the mass balance. Price et al. (2000) obtained good data on the volatile content of Jericho kimberlite, which is shown in Figure 2. Sleep (2003b), using the mantle abundance of Saal et al. (2002), showed that the kimberlite has 2500 times the volatile concentration of normal mantle. The kimberlite's volume was a few cubic kilometers so it could restore the volatile content of $\sim 10^4$ km^3 of lithospheric mantle. The equivalent cube is 20 km on a side. Given that numerous kimberlites occur within well-mapped cratons and that many kimberlites may intrude deep in the lithosphere without seeing the light of day, metasomatism by kimberlites may have significant effects on the rheology of the lithosphere. The effect would be most pronounced if the kimberlites, like Jericho, formed stockworks near the top of the rheological boundary layer, rather than higher up where the lithosphere is cold and rigid.

3.3. Continent-Continent Collisions and Low-Angle Subduction

Cratonal lithosphere faced another episodic danger: wholesale entrainment by subduction (Lenardic et al. 2003). The danger has lurked since the cratons formed in the Archean. All cratonal fragments that do not have modern break-up margins have ancient collisional margins (Bleeker 2003).

Chemical buoyancy provides little protection for the lithosphere entering a subduction zone. As I noted, a 490 K temperature contrast would overwhelm the probable thermal buoyancy. As the whole lithosphere is involved in subduction, this contrast is easily exceeded. Wholesale entrainment occurred in Lenardic et al.'s (2003) models even when they increased the chemical buoyancy to 200 kg m^{-3}.

Lenardic et al. (2003) used yield stress expressed as an effective friction coefficient to parameterize the rheology for subduction. Using numerical modeling, they calculated that the friction coefficient in the cratonal lithosphere needs to be at least twice that of normal mantle. The physics are analogous to a chain: If the

weakest link breaks, we do not find out about the other links if they are moderately stronger.

Conversely, cratonal mantle lithosphere is not inviolate. Low-angle subduction led to its demise beneath West China (Gao et al. 2002) and Wyoming (Canil et al. 2003). Cratonal lithosphere also had to deform to get implaced originally. Quantification of these processes would yield a maximum viscosity and yield stress to go with the minimum ones obtained by considering its long-term survival.

3.4. Platform Subsidence

Archean cratons have typically neither been deeply eroded nor deeply buried since they stabilized after their formation (Galer & Mezger 1998). Sedimentary basins often occur within younger stable platforms to depths of a few kilometers (Figure 1). This distinction seems true, even though there are not enough examples for meaningful statistics. Exposure of the basement alone is a poor criterion. Shallow sediments covered much of the Canadian Shield in the Paleozoic (Patchett et al. 2004). The straightforward inference is that the lithospheric mantle of cratons did not change much once they formed and therefore the freeboard from Equation 5 did not change much. There are additional dynamic inferences related to the subsidence of platforms and the persistence of near sea-level surfaces.

An attractive hypothesis is that chemical buoyancy is important within Archean cratonal lithosphere but not within younger platform lithosphere (Figure 7). We live in a time where the mantle has just cooled enough that platform lithosphere is almost as thick as cratonal lithosphere. Equivalently, the chemically buoyant region of the cratonal lithosphere is now above the regional boundary layer and no longer affects convection.

I present a simple example relevant to Phanerozoic subsidence. The abiabatic mantle has cooled 25 K in the last 500 Ma. From Equation 9 using $T_\eta = 60$ K, platform lithosphere was 87% of its current thickness at 500 Ma. Note that deep crustal xenoliths indicate similar geotherms beneath stable platform and craton in southern Africa from 0.6–0.8 Ga to the Jurassic (Schmitz & Bowring 2003). These data would not resolve a 13% difference in mantle geotherm. For a present 200-km thickness, the 500-Ma thickness was 174 km. This cooling would have produced 500 m of subsidence beneath air. It would have produced 1.9 km of subsidence relative to cratons in a basin filled with 2500-kg m^{-3} sediments. This simple example demonstrates the feasibility of the hypothesis.

Viewed locally, platforms include a few kilometer-deep basins as well as more regional regions of subsidence. The platform basins were not far from active margins. Lithospheric stretching within isolated basins like Michigan is not evident but cannot be excluded outright. Buoyant plume material may pond beneath locally thin lithosphere either from stretching or from having platforms adjacent to thicker cratonal lithosphere. The ponded plume material then may heat and convectively thin nonbuoyant platform lithosphere. Later the platform lithosphere cools back toward its steady-state geotherm and subsides. The subsidence of interior platform

basins is thermal, but is a 2- or 3-dimensional process that is more complicated than vertical cooling of oceanic lithosphere (Kaminski & Jaupart 2000).

A second aspect of this hypothesis is that the mechanical difference between platforms and cratons is waning. One might expect that rifted margins were more likely to crack cratons as we approach the present. There are obvious examples in the North and South Atlantic and Indian Oceans where cratons have recently rifted (Bleeker 2003), but there may not be enough examples and a good enough ancient record for statistical analysis.

3.5. Freeboard and Life

The force available to drive continental tectonics provides a long-term control on continental freeboard (England & Bickle 1984). In particular, forces driving compressional tectonics need to overcome the forces from the tendency of buoyant crust and mantle to spread over more-dense normal mantle like oil over water. Physically, the tendency of continents to spread is proportional to the geoid height and stress resultant in Equation 6. The stress-resultant F is the integral of membrane stress (horizontal stress minus vertical lithostatic stress) over depth. The ridge axis makes a good reference (as used in Equation 6) for zero membrane stress because its hot rocks are weak.

The stress in continental stable interiors has fluctuated between compression and tension over the past 2.6 billion years. Dike swarms are obvious evidence of tension. The Canadian Shield is now under compression (Zoback & Zoback 1997). The 1935 magnitude 6 Timiskaming earthquake is an example of thrust reactivation of part of the early Paleozoic Ottawa (extensional) graben system (Bent 1996).

Over time, stable cratons experience both compression and tension, just like orogens. The effects of compressional and tensional tectonics would balance over time for a region near sea level, which happens to be their actual elevation. Tectonics in the absence of surface processes would maintain elevations near present sea level, although the surface would be rugged. Intriguingly, the Earth has the right amount of ocean water so that tectonics and erosion/deposition both tend to maintain a surface near sea level. This allows the Earth to have shallow continental seas and low-lying dry land, unlike Mars, which always had too little water, or the Jovian satellite Europa, which is covered by a thick ocean. Platforms are not expected on an Earth-sized planet in general as the actual Earth accreted violently and much water was lost in the Moon-forming impact.

The shallow seas that covered North America in the Paleozoic teemed with life, as evidenced by the fossils of organisms that now fill paleontology collections. Shallow seas and adjacent lowlands were the first foothold for land life. But does having the right amount of water affect planetary habitability in general? Enough to seriously think about it.

There would be little erosion on a water-covered world. Hydrothermal circulation would buffer the oceans, as happens to some extent on the present Earth.

The phosphorus supply is then problematic. Both low-temperature and high-temperature hydrothermal circulation through the oceanic crust are sinks (Wheat et al. 1996). The continents are the source of phosphorus, which would be absent without erosion. Phosphorus is a necessary building block of terrestrial life in DNA, for example. Life would have to evolve an efficient means of extracting phosphorus from oceanic basalt to be plentiful.

Conversely, tectonics on a world with less standing water than the Earth has would be different, although a biologically limiting process is not evident. Rivers would plunge into the ocean basins. Sediment would sink to the seafloor where it would eventually be subducted. The absence of stable basins to trap carbonate would be a major effect. The ridge axis would be exposed to the air where ferrous iron in basalt would be a major oxygen sink.

4. CONCLUDING REMARKS

Mantle xenoliths provide data with sufficient time and depth resolution that the results are highly useful for geodynamics. To the first order, chemically buoyant lithosphere formed in the Archean and in many places remained stable after its overlying crust stabilized. The lithospheric thickness in both Archean cratons and younger stable platforms is typically ∼200 km, except where modern tectonics has caused thinning.

Cratonal lithosphere formed by processes similar to modern tectonics including subduction. Seeking a single formation mechanism is misguided. Large-extent partial melting at high temperatures produced its buoyant and refractory character. Yet most of the mantle that contributed melts to the crust did not end up as cratonal keels. Conversely, the Archean continental crust formed by processes above hot mantle that resemble modern tectonics. The most controversial aspect is vertical tectonics because the modern analog is not well understood and because the effects of hot ponded plume material beneath the lithosphere were more profound in the Archean.

The end of the Archean at ∼2500 Ma marks a change in the Earth's tectonics. Cooling of the Earth's interior is one part of the story; much of the rest is that sizable continents existed by 2500 Ma. As at the present, continents modulated tectonics on a global scale (Lowe 1992). Archean cratons have survived numerous break-up and collision events (Bleeker 2003). Otherwise modulation of plate tectonics by continents is beyond the scope of this review.

The latter history of cratons is stability both at the surface and down to near the base of the lithosphere. In contrast to most geodynamics, I am left to explain why very little happened. The high viscosity, yield strength, and buoyancy contributed to the stability of cratonal lithospheric mantle. However, the rheological boundary layer beneath the lithosphere was active. That is, stagnant-lid convection in the underlying normal mantle supplied the conductive heat flow to the surface. The chemical lithosphere survived being entrained both as wisps in convective

downwelling and wholesale by continental collisions. It failed to survive low-angle subduction beneath Wyoming and North China.

Platforms are younger stable regions where chemically buoyant lithosphere does not affect convection (Figure 7). Platform lithosphere has thickened over time as the Earth's interior has cooled. The cooling in the past 500 Ma produced ∼500 m of subsidence beneath air, enough for platforms to subside preferentially to cratons. At present, platform lithosphere is almost as thick as cratonal lithosphere. As the Earth cools further, the chemically buoyant region of cratonal lithosphere will be too shallow to affect convection. The geodynamic differences between platforms and cratons will become less pronounced.

ACKNOWLEDGMENTS

**The *Annual Review of Earth and Planetary Science* is online at
http://earth.annualreviews.org**

LITERATURE CITED

Abbott DL, Burgess L, Longhi J, Smith WHF. 1994. An empirical thermal history of the Earth's upper mantle. *J. Geophys. Res.* 99: 13835–50

Arndt N. 2003. Komatiites, kimberlites, and boninites. *J. Geophys. Res.* 108: doi: 10.1029/2002JB002157

Artemieva IM, Mooney WD, 2001. Thermal thickness and evolution of Precambrian lithosphere: a global study. *J. Geophys. Res.* 106: 16387–414

Bédard JH, Brouillette P, Madore L, Berclaz A. 2003. Archaean cratonization and deformation in the northern Superior Province, Canada: an evaluation of plate tectonic versus vertical tectonic models. *Precambrian Res.* 127:61–87

Bell DR, Schmitz MD, Janney PE. 2003. Mesozoic thermal evolution of the southern African mantle lithosphere. *Lithos* 71:273–87

Bent AL. 1996. An improved source mechanism for the 1935 Timiskaming, Quebec earthquake from regional waveforms. *Pure Appl. Geophys.* 146:5–20

Bleeker W. 2003. The late Archean record: a puzzle in ca. 35 pieces. *Lithos* 71:99–134

Boyd FR, Gurney JJ, Richardson SH. 1985. Evidence for a 150–200 km thick Archean lithosphere from diamond inclusion thermobarometry. *Nature* 315:387–89

Brey GP, Köhler T, 1990. Geothermobarometry in four-phase lherolites. II. New thermobarometers and practical assessment of existing thermobarometers. *J. Petrol.* 31:1353–78

Burke K, Kidd WSF. 1978. Were Archean continental geothermal gradients much steeper than those of today? *Nature* 272:240–41

Canil D, Schulze DJ, Hall D, Hearn BC Jr, Milliken SM. 2003. Lithospheric roots beneath western Laurentia: the geochemical signal in mantle garnets. *Can. J. Earth Sci.* 40:1027–1051

Carlson RW, Pearson DG, Boyd FR, Shirey SB, Irvine G, et al. 1999. Re-Os systematics of lithosphere peridotites: implications for lithosphere formation and preservation. In *Proc. 7th Int. Kimberlite Conf., The J. B. Dawson Volume*, ed. JJ Gurney,

JL Gurney, MD Pascoe, SH Richardson, pp. 117–24. Cape Town: Red Roof Design. 493 pp.

Chen SF, Witt WK, Liu SF. 2001. Transpression and restraining jogs in the northeastern Yilgarn craton, Western Australia. *Precambrian Res.* 106:309–28

Chesley JT, Rudnick R, Lee C-T. 1999. Re-Os systematics of mantle xenoliths from the East African Rift: age, structure, and history of the Tanzanian craton. *Geochim. Cosmochim. Acta* 63:1203–17

Choblet G, Sotin C. 2000. 3D thermal convection with variable viscosity: Can transient cooling be described by a quasi-static scaling law. *Phys. Earth Planet. Inter.* 119:321–36

Chulick GS, Mooney WD. 2002. Seismic structure of the crust and uppermost mantle of North America and adjacent oceanic basins: a synthesis. *Bull. Geol. Soc. Am.* 92:2478–92

Davaille A, Jaupart C. 1993a. Thermal convection in lava lakes. *Geophys. Res. Lett.* 20: 1827–30

Davaille A, Jaupart C. 1993b. Transient high-Rayleigh-number thermal convection with large viscosity variations. *J. Fluid Mech.* 253:141–66

Davaille A, Girard F, Le Bars M. 2002. How to anchor hot spots in a convecting mantle? *Earth Planet. Sci. Lett.* 203:621–34

Davis WJ, Canil WJ, MacKenzie JM, Carbno GB. 2003a. Petrology and U-Pb geochronology of lower crust xenoliths and the development of a craton, Slave Province, Canada. *Lithos* 71:541–73

Davis WJ, Jones AG, Bleeker W, Grütter H. 2003b. Lithospheric development in the Slave craton: a linked crustal and mantle perspective. *Lithos* 71:575–89

de Ronde CEJ, Kamo SL. 2000. An Archean arc-arc collision event: a short-lived (Ca 3 Myr) episode, Weltevreden area, Barbarton greenstone belt, South Africa. *J. Afr. Earth Sci.* 30:219–48

de Ronde CEJ, de Wit MJ. 1994. Tectonic history of the Barberton greenstone belt, South Africa: 490 million years of Archean crustal evolution. *Tectonics* 13:983–1005

Doin M-P, Fleitout L, Christensen U. 1997. Mantle convection and stability of depleted and undepleted continental lithosphere. *J. Geophys. Res.* 102:2771–87

England P, Bickle M. 1984. Continental thermal and tectonic regimes during the Archean. *J. Geol.* 92:353–67

Farquhar J, Wing BA, McKeegan KD, Harris JW, Cartigny P, Thiemens MH 2002. Mass-independent sulfur of inclusions in diamond and sulfur recycling on the early Earth. *Science* 298:2369–72

Fei Y, Bertka CM, Mysen BO, eds. 1999. *Mantle Petrology*: *Field Observations and High Pressure Experimentation: A Tribute to Francis R.* (*Joe*) *Boyd*. Houston: Geochem. Soc., Spec. Publ. 6, 322 pp.

Fiorentini G, Lissia M, Mantovani F, Vannucci R. 2003. Geo-neutrinos, mantle circulation and silicate earth. *J. High Energy Part. Phys, Valencia 2003, Astroparticle and high energy physics*: AHEP2003/035 hep-ph0401085

Francis D. 2003. Cratonic mantle roots, remnants of a more chondritic Archean mantle. *Lithos* 71:135–52

Galer SJG, Mezger K. 1998. Metamorphism denudation and sea level in the Archean and cooling of the Earth. *Precambrian Res.* 92: 387–412

Gao S, Rudnick RL, Carlson RW, McDonough WF, Liu YS. 2002. Re-Os evidence for replacement of ancient mantle lithosphere beneath the North China craton. *Earth Planet. Sci. Lett*. 198:307–22

Griffin WL, O'Reilly SY, Ryan CG. 1999. The composition and origin of sub-continental mantle. See Fei et al. 1999, pp. 13–45

Griffin WL, O'Reilly SY, Abe N, Aulbach S, Davies RM, et al. 2003a. The origin and evolution of Archean lithospheric mantle. *Precambrian Res.* 127:19–41

Griffin WL, O'Reilly SY, Natapov LM, Ryan CG. 2003b. The evolution of the lithospheric mantle beneath the Kalahari Craton and its margins. *Lithos* 71:215–41

Grove TL, Parman SW. 2004. Thermal evolution of the Earth as recorded by komatiites. *Earth Planet. Sci. Lett.* 219:173–87

Heaman LM, Kjarsgaaed BA, Creaser RA. 2003. The timing of kimberlite magmatism in North America: implications for global kimberlite genesis and diamond exploration. *Lithos* 71:153–84

Herzberg C. 1999. Phase equilibrium constraints on the formation of cratonic mantle. See Fei et al. 1999, pp. 241–57

Hoal KO. 2003. Samples of Proterozoic iron-enriched mantle from the Premier kimberlite. *Lithos* 71:259–72

Heubeck C, Lowe DR. 1994. Late syndepositional deformation and detachment tectonics in the Barberton Greenstone Belt, South Africa. *Tectonics* 13:1514:36

Irvine GJ, Pearson DG, Kjarsgaard BA, Carlson RW, Kopylova MG, Dreibus G. 2003. A Re-Os isotope and PGE study of kimberlite-derived peridotite xenoliths from Somerset Island and a comparison to the Slave and Kaapvaal cratons. *Lithos* 71:461–88

Jacob DE, Schmickler B, Schulze DJ. 2003. Trace element geochemistry of coesite-bearing eclogites from the Roberts Victor kimberlite, Kaapvaal craton. *Lithos* 71: 337–51

Jacobsen SB. 1988. Isotopic constraints on crustal growth and recycling. *Earth Planet. Sci. Lett.* 90:315–29

Jones AG, Carlson H, Grütter A, eds. 2003. A tale of two cratons; the Slave-Kaapvaal Workshop. *Lithos* 71:99–596

Kaminski E, Jaupart C. 2000. Lithospheric structure beneath the Phanerozoic intracratonal basins of North America. *Earth Planet. Sci. Lett.* 178:139–49

Kisters AFM, Stevens G, Dziggel A, Armstrong RA. 2003. Extensional detachment faulting and core-complex formation in the southern Barberton granite-greenstone terrain, South Africa: evidence for a 3.2 Ga orogenic collapse. *Precambrian Res.* 127:355–78

Kiyokawa S, Taira A, Bryrne T, Bowring S, Sano Y. 2002. Structural evolution of the middle Archean coastal Pilbara Rerrane, Western Australia. *Tectonics* 21: doi: 10.1029/2001TC001296

Kopylova MG, Russell JK, Cookenboo H. 1999. Petrology of peridotite and pyroxenite xenoliths from the Jericho kimberlite: implications for the thermal state of the mantle beneath the Slave craton: Northern Canada. *J. Petrol.* 40:79–104

Lenardic A, Moresi L. 2003. Thermal convection below a conducting lid of variable extent: heat flow scalings and two-dimensional, infinite Prandtl number numerical simulations. *Phys. Fluids* 15:455–66

Lenardic A, Moresi L-N, Mühlhaus H. 2003. Longevity and stability of cratonic lithosphere: insights from numerical simulations of coupled mantle convection and continental tectonics. *J. Geophys. Res.* 108:doi: 10.1029/2002JB001859

Lowe DR. 1992. Major events in the geological development of the Precambrian Earth. In *The Proterozoic Biosphere, A Multidisciplinary Study*, ed. JW Schopf, C Klein, 2.7:67–73. New York: Cambridge Univ. Press. 1348 pp.

McLennan SM, Taylor SR. 1991. Sedimentary-rocks and crustal evolution—Tectonic setting and secular trends. *J. Geol.* 99:1–21

Menzies AH, Carlson RW, Shirey SB, Gurney JJ. 2003. Re-Os systematics of diamond-bearing eclogites from the Newlands kimberlite. *Lithos* 71:323–36

Mooney WD, Vidale JE. 2003. Thermal and chemical variations in subcrustal cratonic lithosphere: evidence from crustal isostasy. *Lithos* 71:185–93

Nyblade AA, Sleep NH. 2003. Long lasting epeirogenic uplift from mantle plumes and the origin of the southern African plateau. *Geochem. Geophys. Geosyst.* 4:1105. doi: 10.1029/2003GC000573

O'Neill CJ, Moresi L. 2003. How long can diamonds remain stable in the continental lithosphere? *Earth Planet. Sci. Lett.* 213:43–52

Patchett PJ, Embry AF, Ross GM, Beauchamp B, Harrison JC, et al. 2004. Sedimentary cover of the Canadian Shield through Mesozoic time reflected by Nd isotopic and geochemical results for the Sverdrup Basin, Arctic Canada. *J. Geol.* 112:39–57

Pavlov A, Kasting JF. 2002. Mass-independent fractionation of sulfur isotopes in Archean sediments: strong evidence for an anoxic Archean atmosphere. *Astrobiology* 2:27–41

Pearson DG. 1999. The age of continental roots. *Lithos* 48:171–94

Price SE, Russell JK, Kopylova MG. 2000. Primitive magma from the Jericho pipe, NWT, Canada: constraints on primary melt chemistry? *J. Petrol.* 41:789–808

Richter FM. 1973. Convection and the large-scale circulation of the mantle. *J. Geophys. Res.* 78:8735–45

Richter FM. 1988. A major change in the thermal state of the Earth at the Archean-Proterozoic boundary: consequences for the nature and preservation of the Archean lithosphere. *J. Petrol. Spec. Lithosphere Issue*, pp. 39–52

Ritsema J, van Heist H. 2000. New seismic model of the upper mantle beneath Africa. *Geology* 28:63–66

Röhm AHE, Snieder R, Goes S, Trampert J. 2000. Thermal structure of continental upper mantle inferred from S-wave velocity and surface heat flow. *Earth Planet. Sci. Lett.* 181:395–407

Rudnick RL, Nyblade AA. 1999. The thickness and heat production of Archean lithosphere: constraints from xenolith thermobarometry and surface heat flow. See Fei et al. 1999, pp. 3–12

Saal AE, Hauri EH, Langmuir CH, Perfitt MR. 2002. Vapour undersaturation in primitive mid-ocean-ridge basalt and the volatile content of the Earth's upper mantle. *Nature* 419:451–55

Saltzer RL, Chatterjee N, Grove TL. 2001. The spatial distribution of garnets and pyroxenes in mantle peridoties: pressure-temperature history of peridotites from the Kaapvaal craton. *J. Petrol.* 42:2231–29

Schmidberger SS, Simonetti A, Francis D, Gariepy C. 2002. Probing Archean lithosphere using the Lu-Hf isotope systematics of periodite xenoliths from Somerset Island kimberlites, Canada. *Earth Planet. Sci. Lett.* 197:245–59

Schmitz MD, Bowring SA. 2003. Constraints on the thermal evolution of continental lithosphere from U-Pb accessory mineral thermochronology of lower crustal xenoliths, southern Africa. *Contrib. Mineral. Petrol.* 144:592–618

Schulze DJ, Harte B, Valley JW, Brenan JM, Channer DM de R. 2003a. Extreme crustal oxygen isotope signatures preserved in coesite in diamond. *Nature* 423:68–70

Schulze DJ, Valley JW, Spicuzza MJ, Channer DM de R. 2003b. The oxygen isotope composition of eclogitic and peridotitic garnet xenoliths from the La Ceniza kimberlite, Guaniamo, Venezuela. *Int. Geol. Rev.* 45:968–75

Shapiro SS, Hager BH, Jordan TH. 1999a. The continental tectosphere and Earth's long-wavelength gravity field. *Lithos* 48:135–52

Shapiro SS, Hager BH, Jordan TH. 1999b. Stability and dynamics of the continental tectosphere. *Lithos* 48:115–33

Shirey SB, Haris JW, Richardson SH, Fouch M, James DE, et al. 2003. Regional patterns in the paragenesis and age of inclusion in diamond, diamond composition, and the lithospheric seismic structure of southern Africa. *Lithos* 71:243–58

Simons FJ, Zielhuis A, van der Hilst RD. 1999. The deep structure of the Australian continent from surface wave tomography. *Lithos* 48:17–43

Sleep NH. 1992. Archean plate-tectonics—what can be learned from continental geology? *Can. J. Earth Sci.* 29:2066–71

Sleep NH. 2003a. Survival of Archean cratonal lithosphere. *J. Geophys. Res.* 108: doi: 10.1029/2001JB000169

Sleep NH. 2003b. Geodynamic implications of xenolith geotherms. *Geochem. Geophys. Geosyst.* 4:1079. doi:10.1029/2003 GC000511

Solomatov VS. 1995. Scaling of temperature- and stress-dependent viscosity convection. *Phys. Fluids* 7:266–74

Solomatov VS, Moresi L-N. 2000. Scaling of time-dependent stagnant lid convection: application to small-scale convection on Earth

and other terrestrial planets. *J. Geophys. Res.* 105:21795–817

Wheat CG, Feely RA, Mottl MJ. 1996. Phosphate removal by oceanic hydrothermal processes: an update of the phosphorus budget in the oceans. *Geochim. Cosmochim. Acta* 60: 3593–608

Zegers TE, de Keijzer M, Passchier CW, White SH. 1998. The Mulgandinnah shear zone: an Archean crustal scale strike-slip zone, eastern Pilbara, Western Australia. *Precambrian Res*. 88:233–47

Zegers TE, Nelson DR, Wilbrans JR, White SH. 2001. SHRIMP U-Pb zircon dating of Archean core complex formation and cratonic deformation in the East Pilbara granite-greenstone terrain. *Tectonics* 20:883–903

Zoback ML, Zoback MD. 1997. Crustal stress and intraplate deformation? *Geowissenschaften* 15:116–23

Contents

ERRATA
  An online log of corrections to *Annual Review of Earth and
  Planetary Sciences* chapters may be found at
  http://earth.annualreviews.org